The diversity of the microbiome impacts chronic lymphocytic leukemia development in mice and humans

Tereza Faitová,[1*] Mariana Coelho,[2,3*] Caspar da Cunha-Bang,[1] Selcen Öztürk,[2] Ece Kartal,[4] Peer Bork,[4-7] Martina Seiffert[2#] and Carsten U. Niemann[1,8#]

[1]Department of Hematology, Rigshospitalet, Copenhagen, Denmark; [2]Department of Molecular Genetics, German Cancer Research Center (DKFZ), Heidelberg, Germany; [3]Faculty of Biosciences of the University of Heidelberg, Heidelberg, Germany; [4]Structural and Computational Biology Unit, European Molecular Biology Laboratory (EMBL), Heidelberg, Germany; [5]Department of Bioinformatics, Biocenter, University of Würzburg, Würzburg, Germany; [6]Yonsei Frontier Lab (YFL), Yonsei University, Seoul, South Korea; [7]Max Delbrück Center for Molecular Medicine, Berlin, Germany and [8]Department of Clinical Medicine, University of Copenhagen, Copenhagen, Denmark

TF and MC contributed equally as first authors.
#MS and CUN contributed equally as senior authors.

Correspondence: C.U. Niemann
carsten.utoft.niemann@regionh.dk

M. Seiffert
m.seiffert@dkfz-heidelberg.de

Received: November 17, 2023.
Accepted: April 30, 2024.
Early view: May 9, 2024.

https://doi.org/10.3324/haematol.2023.284693

The Diversity of the Microbiome Impacts Chronic Lymphocytic Leukemia Development in Mice and Humans - Supplemental Methods and Supplemental Figures

*Tereza Faitová[1], *Mariana Coelho[2,3], Caspar da Cunha Bang[1], Selcen Öztürk[2], Ece Kartal[4], Peer Bork[4,5,6,7], #Martina Seiffert[2], #Carsten U. Niemann[1,8]

Affiliations

[1] Department of Hematology, Rigshospitalet, Copenhagen, Denmark

[2] Department of Molecular Genetics, German Cancer Research Center (DKFZ), Heidelberg, Germany

[3] Faculty of Biosciences of the University of Heidelberg, Heidelberg, Germany

[4] Structural and Computational Biology Unit, European Molecular Biology Laboratory (EMBL), Heidelberg, Germany

[5] Department of Bioinformatics, Biocenter, University of Würzburg, Würzburg, Germany

[6] Yonsei Frontier Lab (YFL), Yonsei University, Seoul, South Korea

[7] Max Delbrück Center for Molecular Medicine, Berlin, Germany

[8] Department of Clinical Medicine, University of Copenhagen, Copenhagen, Denmark

Co-first/co-senior authorship

*/# These authors contributed equally to this work

Content

1. Supplemental Methods

Animal models

Eμ-TCL1 (TCL1) mice on a C57BL/6 J background were kindly provided by Carlo M. Croce (The Ohio State University, Columbus, Ohio, USA), and crossed at least 10 times to ensure C57BL/6 J background (1). 6-8 week old female C57BL/6 J mice for adoptive transfer (AT) of TCL1 tumors were bred and maintained at the central animal facility of the German Cancer Research Center (DKFZ, Heidelberg).

Two colonies of C57BL/6 mice were maintained in two different animal facilities of the German Cancer Research Center (DKFZ) – a low hygiene facility, without user-entry restrictions, and a high hygiene facility (where altered Schaedler flora was ensured). Mice were kept on the same water and food restrictions on both facilities. Ten 7-week-old mice from each colony were submitted to adoptive transfer (AT) with leukemia cells from the TCL1 mouse model (TCL1 AT), as previously described (2, 3). In short, splenocyte suspensions obtained from 40-60 week-old female TCL1 mice underwent B cell purification with the EasySep Mouse Pan-B Cell Isolation Kit (StemCell Technologies Inc., 19844) according to manufacturer instructions. The tumor content (percentage of CD5+CD19+ cells) post-purification reached 95% or higher, according to flow cytometry (FC) measurement. 2x107 cells were injected intraperitoneously, and animals were monitored for the development of leukemia, through weekly blood withdrawals starting at week 2 post-transplantation. Leukemic animals were identified given the presence of a growing CD5+CD19+ tumor population in the blood (as measured by FC), as well as palpable splenomegaly. 3 mice were removed from the study upon failing in tumor engraftment.

Murine samples collection, DNA extraction and sequencing

Fecal samples were collected at week 0, one day before TCL1 AT, and at week 3 post-transplantation (after tumor was established), into Stool Nucleic Acid Collection and Preservation System tubes (Norgen Biotek, 63700). Fecal samples were snap-frozen with liquid N2 immediately after collection. QIAmp DNA Stool Mini Kit (Qiagen, Hilden, Germany) was used to extract DNA from fecal samples according to manufacturer instructions. The concentration of DNA was determined by NanoDrop spectrophotometry (NanoDrop, Germany). In short, 50 mg of fecal sample was lyophilized in 400 µL extraction buffer (methanol/ddH2O at a ratio of 4/1). Sample mixture was grinded for 6 minutes and sonicated at 5 ºC for 30 minutes. Mixture was then kept at -20 ºC for 30 minutes and centrifuged at 13,000 g and 4 ºC for 15 minutes. Supernatant was collected and snap-frozen. Snap-frozen sample was re-dissolved in 100 µL 90% methanol (in ddH2O). Quality control sample was prepared for NanoDrop measurement. Shotgun sequencing was conducted at the European Molecular Biology Laboratory (EMBL, Heidelberg) on Illumina HiSeq 4000 platform in a 2x150bp paired-end setup at the Genomics Core Facility, European Molecular Biology Laboratory in Heidelberg, Germany.

Peripheral blood (PB) was drawn from the submandibular vein for weekly measurements, and collected in ethylenediaminetetraacetic acid (EDTA)-coated tubes (Sarstedt) for immunostaining and FC measurement. Mice were euthanized by increasing concentrations of carbon dioxide (CO2). Single-cell suspensions from spleen, bone marrow (BM) and inguinal lymph nodes (LN) were prepared as described previously (2, 3). Briefly, splenocyte suspensions were generated with the GentleMACS tissue dissociator (Miltenyi Biotec), followed by red blood cell (RBC) lysis, and passing the cells by 70-µm strainers (BD Biosciences) to exclude fat and cell clumps. BM cells were flushed from femurs with PBS/2% fetal calf serum (FCS). LN cell suspensions were prepared through grinding the lymph nodes through 70-µm strainers (BD Biosciences).

Flow cytometry

All antibodies were purchased from BD, Biolegend or ThermoFisher Scientific. For surface staining, single-cell suspensions previously obtained were washed with PBS/2% FCS, and incubated with recommended antibodies against cell surface markers, using the respective recommended antibody dilutions. Incubation went on for 30 minutes, at 4 ºC in the dark. After washing twice with PBS/2% FCS, cells were fixed using IC fixation buffer (ThermoFisher Scientific, 00-8222-49), washed and stored in PBS/2% FCS at 4ºC in the dark until analyzed by FC.

For intracellular staining with FoxP3, cells were fixed after surface staining using FoxP3 fixation/permeabilization buffer (ThermoFisher Scientific, 00-552300) for 30 minutes at RT (in the dark). Then, permeabilization was performed with 1X permeabilization buffer (ThermoFisher Scientific, 00-5523-00) and staining with antibody against FoxP3 transcription factor in 1X permeabilization buffer was started for 30 minutes at 4 ºC. after two washes with 1X permeabilization buffer, cells were resuspended in the same buffer and stored at 4 ºC in dark conditions, until analyzed by FC.

For PB staining, 25 µL of blood were stained with surface molecule antibodies for 30 minutes at 4 ºC in the dark. Then, blood samples were incubated for 10 minutes in 2 mL of 1X 1-step Fix/Lyse Solution (ThermoFisher Scientific, 00-5333-57) for RBC removal. After centrifugation and discarding of the supernatant, cell pellets were resuspended in PBS. Less than 1 hour before FC measurement, 25 µL of 123count eBeads (ThermoFisher Scientific, 01-1234-42) were added, to allow calculation of absolute number of cells in the blood according to the formula: absolute count (cells/µL) = (cell count x bead volume x bead concentration)/(bead count x cell volume).

Flow cytometry data acquisition was done using BD LSRFortessa flow cytometer (BD Biosciences). For analysis, dead cells and doublets were excluded. Median Fluorescence Intensity (MFI) was calculated and normalized by subtracting the MFI of the respective fluorescence minus one (FMO) control, for markers without a clear negative vs positive population distinction. Data analysis was performed using FlowJo X 10.0.7 software (FlowJo LLC, BD Biosciences).

Patient cohort and patient data

Fecal samples were collected from 60 patients enrolled in the CLL biobank and the PERSIMUNE biobank during regular out-patient visits at Rigshospitalet, Copenhagen, Denmark, between June 2017, and July 2020. The project was approved by the national ethics committee (approval no. 1804410) and written informed consent was obtained from all patients prior to sampling.

Patient sample collection and sequencing

Fecal samples were collected by the patient or nursing staff using the OMNIgene.GUT (DNA Stabilized-frozen Inc., Ottawa, ON, Canada) stabilization tube according to the manufacturer's instructions and refrigerated for a maximum of 7 days before freezing at -80 C. All samples were processed and stored at the PERSIMUNE biobank located at Rigshospitalet. Samples were extracted from the biobank and transported on dry ice to the IrsiCaixa AIDS Research Institute, Spain. Here samples were thawed on ice and DNA was extracted from ~200 mg of each fecal sample using the Power Soil DNA Extraction Kit (MO BIO Laboratories, Carlsbad, CA, US). 4 Extracted DNA was then stored at -80 ºC until sequencing. For sequencing, whole fecal DNA was chemically fragmented using the Nextera-XT® Illumina kit. Total fecal DNA was sequenced on an Illumina Hi-Seq® platform in a 2x150bp paired-end setup.

Preprocessing and taxonomical profiling

Both, reads preprocessing and taxonomical profiling were done for the mouse and CLL samples using an in-house pipeline implemented in ngless (4). After sequencing, reads underwent quality control and preprocessing steps, including trimming of reads using a quality score cutoff of 20, and removal of reads below 100 base pairs. Reads were mapped to the mouse and human genomes (mm39 and hg19, respectively) using BWA-MEM2 (5) and reads with a minimum identity of 80 across 90 bases were discarded. Gene profiling was carried out by mapping to the integrated gene catalogue (IGC) (6) with BWA-MEM2 and counting the number of reads mapping to each gene with a minimum match size of 60 and minimum identity of 90. Taxonomic profiling and estimation of the relative abundances at all taxonomical levels in mice and humans were done using mOTUs2 (7) and reference-independent method MetaPhlAn3 (8), respectively. The naming for mOTUs gives all possible species that the specific mOTU potentially represents. The format is species1/species2/species3/etc., meaning that all the species are possible annotations. MetaPhlAn3 utilizes the marker gene database to align the metagenomic sequencing data. By identifying the most suitable marker gene sequences, MetaPhlAn3 ensures a unique species assignment during the alignment of metagenomic sequencing data to the marker gene database. Taxa failing to be classified into any taxonomic ranks were marked as *Unclassified* by both mOTUs2 and MetaPhlAn3.

Bioinformatics and Statistical analysis

Statistical analyses of FC mouse data were performed using GraphPad Prism software version 9. All graphs show means ± SEM, unless otherwise indicated. Comparisons of two different sample groups (n = 8, n = 9) at each blood withdrawal timepoint were performed using a non-parametric Mann Whitney t-test. All other statistical analyses were performed using R (version 4.2.0).

Descriptive analyses were performed for both the mouse and human CLL cohorts with relative bacterial abundance as input data. Unless stated otherwise, Mann Whitney U Test (Wilcoxon Rank Sum Test) was used to identify significant differences between subgroups; Benjamini-Hochberg (BH) method was used for multiple-testing correction; BH adjusted p-value of <0.05 was considered significant. PERMANOVA (*adonis2* from *vegan* R package version 2.6-2) was used to test statistical differences in microbial composition among different groups of murine samples (such as cage effect) or groups of patient samples (such as gender, groups patients with different antibiotic usage, or resulting patient clusters).

Alpha diversity measures (richness, Shannon index) were calculated at species level using *vegan* R package version 2.6-2 (9). Generalized linear model (GLM) was used to visualize relationship between two independent binary variables - TCL1 AT and hygiene of the animal facilities, and one dependent variable - bacterial relative abundance. Interpretation of the GLM statistical analysis is detailed in Figure 6C legend.

The interindividual dissimilarities in gut microbiota composition (β-diversity) in patients with CLL were assessed by robust aitchison dissimilarity index (*vegdist* function from *vegan* R package version 2.6-2). Hierarchical clustering (*hclust* from base R package *stats*) with Ward's minimum variance method was run on the distance matrix. The interindividual dissimilarities represented by the distance matrix and the formed clusters were visualized using Principal Coordinate Analysis (PCoA, *gl.pcoa* function from *dartR* R package version 2.7.2) (10). First 3 components of PCoA were visualized using 3D plot as Figure 1B (*scatter3D* function from *plot3D* graphics library in R, version 1.4). Statistical differences in microbial composition given by β-diversity estimates between the resulting cluster were tested using PERMANOVA.

Differential abundance of bacterial species in fecal microbiome between CLL patient clusters was assessed using the R implementation of SIAMCAT (*SIAMCAT* R package version 2.0.0) (11). The cutoff value for bacterial taxa to be considered differentially abundant was log fold change > 1 (logFC).

R script as well as taxonomical profiling data of the mice cohort are available at https://github.com/PERSIMUNE/PAC2023Faitova_Human_Mice_CLL.

2a. R Shiny applications – Methods

Relative bacterial abundance and GMM abundance data from individual patient samples were retrieved as described in main Methods section. Relative bacterial abundance data refers to information about the proportional representation of different bacterial species or taxa within a given sample. GMM abundance represents a normalized proxy for the portion of bacteria in a sample that have the ability to perform a specific function. Graphs representing the abundances were constructed using ggplot2 package in R (version 3.3.6). Interactive features such as tooltips, zooming, panning, and hover effects were introduced to the static ggplot2 graphs using plotly package (version 4.10.0). The *ggplotly* function was employed to convert the ggplot2 graphs into interactive plotly graphs.

The R Shiny framework is employed to develop interactive web applications which were deposited on the open source Shinyapps.io. The applications are accessible through links that can be found in the main text.

2b. R Shiny applications – Tutorial

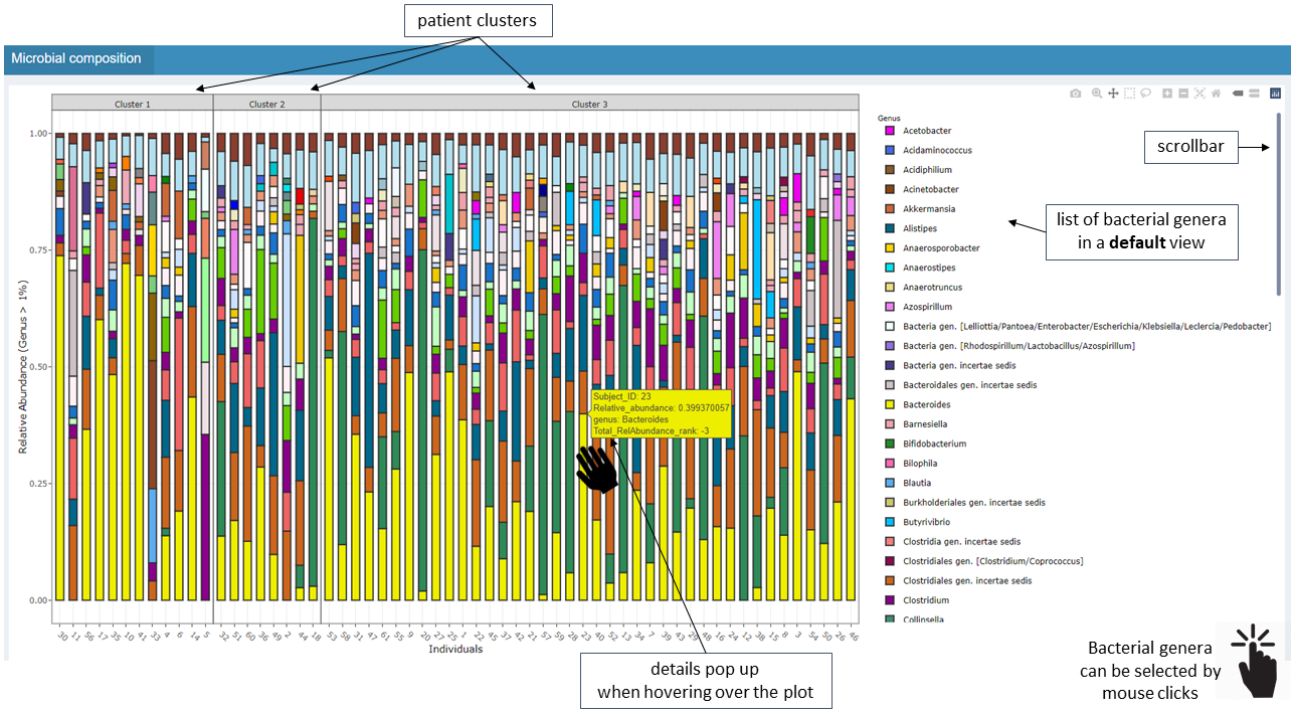

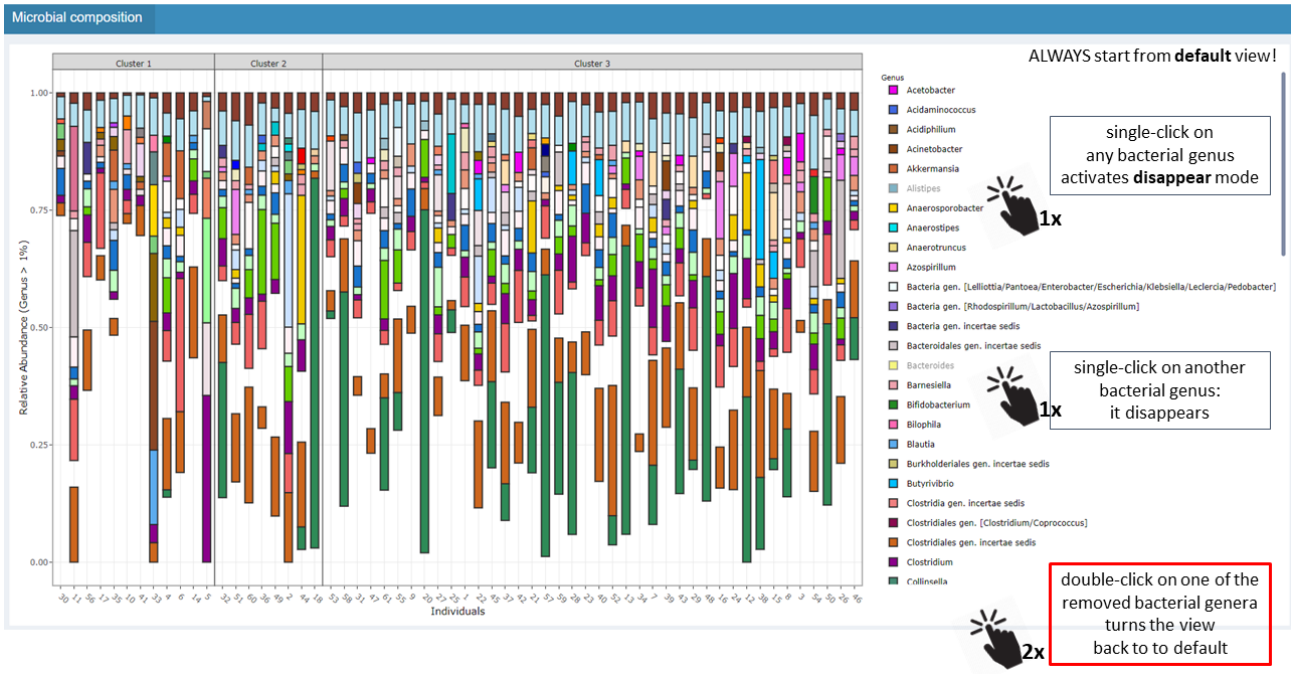

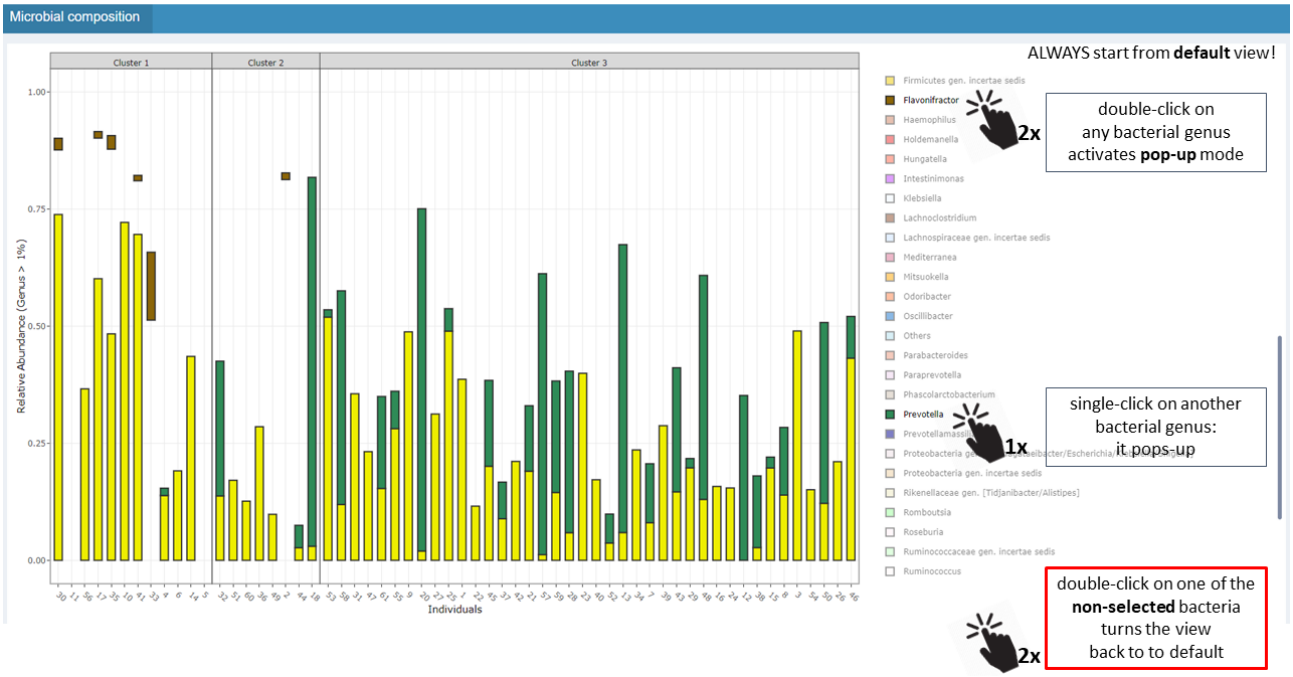
Microbial composition
Cluster 1
Cluster 2
Cluster 3
Relative Abundance (Genus > 1%)
1.00
0.75
0.50
0.25
0.00
Individuals
ALWAYS start from **default** view!
Firmicutes gen. incertae sedis
Flavonifractor
Haemophilus
Holdemanella
Hungatella
Intestinimonas
Klebsiella
Lachnoclostridium
Lachnospiraceae gen. incertae sedis
Mediterranea
Mitsuokella
Odoribacter
Oscillibacter
Others
Parabacteroides
Paraprevotella
Phascolarctobacterium
Prevotella
Proteobacteria gen. incertae sedis
Rikenellaceae gen. [Tidjanibacter/Alistipes]
Romboutsia
Roseburia
Ruminococcaceae gen. incertae sedis
Ruminococcus
2x
double-click on any bacterial genus activates **pop-up** mode
1x
single-click on another bacterial genus: it pops-up
2x
double-click on one of the **non-selected** bacteria turns the view back to to default

References

1. Bichi R, Shinton SA, Martin ES, Koval A, Calin GA, Cesari R, et al. Human chronic lymphocytic leukemia modeled in mouse by targeted TCL1 expression. Proc Natl Acad Sci U S A. 2002;99(10):6955-60.
2. Hanna BS, McClanahan F, Yazdanparast H, Zaborsky N, Kalter V, Rossner PM, et al. Depletion of CLL-associated patrolling monocytes and macrophages controls disease development and repairs immune dysfunction in vivo. Leukemia. 2016;30(3):570-9.
3. McClanahan F, Hanna B, Miller S, Clear AJ, Lichter P, Gribben JG, et al. PD-L1 checkpoint blockade prevents immune dysfunction and leukemia development in a mouse model of chronic lymphocytic leukemia. Blood. 2015;126(2):203-11.
4. Coelho LP, Alves R, Monteiro P, Huerta-Cepas J, Freitas AT, Bork P. NG-meta-profiler: fast processing of metagenomes using NGLess, a domain-specific language. Microbiome. 2019;7(1):84.
5. Li H, Durbin R. Fast and accurate short read alignment with Burrows-Wheeler transform. Bioinformatics. 2009;25(14):1754-60.
6. Li J, Jia H, Cai X, Zhong H, Feng Q, Sunagawa S, et al. An integrated catalog of reference genes in the human gut microbiome. Nature Biotechnology. 2014;32(8):834-41.
7. Milanese A, Mende DR, Paoli L, Salazar G, Ruscheweyh H-J, Cuenca M, et al. Microbial abundance, activity and population genomic profiling with mOTUs2. Nature Communications. 2019;10(1):1014.
8. Beghini F, McIver LJ, Blanco-Míguez A, Dubois L, Asnicar F, Maharjan S, et al. Integrating taxonomic, functional, and strain-level profiling of diverse microbial communities with bioBakery 3. Elife. 2021;10.
9. Oksanen J SG, Blanchet F, Kindt R, Legendre P, Minchin P, O'Hara, R SP, Stevens M, Szoecs E, Wagner H, Barbour M, Bedward M,, Bolker B BD, Carvalho G, Chirico M, De Caceres M, Durand S,, Evangelista H FR, Friendly M, Furneaux B, Hannigan G, Hill M,, Lahti L MD, Ouellette M, Ribeiro Cunha E, Smith T, Stier A, Ter, Braak C WJ. _vegan: Community Ecology Package_. In: package R, editor. 2022.
10. Gruber B, Unmack PJ, Berry OF, Georges A. dartr: An r package to facilitate analysis of SNP data generated from reduced representation genome sequencing. Mol Ecol Resour. 2018;18(3):691-9.
11. Wirbel J, Zych K, Essex M, Karcher N, Kartal E, Salazar G, et al. Microbiome meta-analysis and cross-disease comparison enabled by the SIAMCAT machine learning toolbox. Genome Biology. 2021;22(1):93.
12. Gacesa R, Kurilshikov A, Vich Vila A, Sinha T, Klaassen MAY, Bolte LA, et al. Environmental factors shaping the gut microbiome in a Dutch population. Nature. 2022;604(7907):732-9.

Supplemental Figure 1

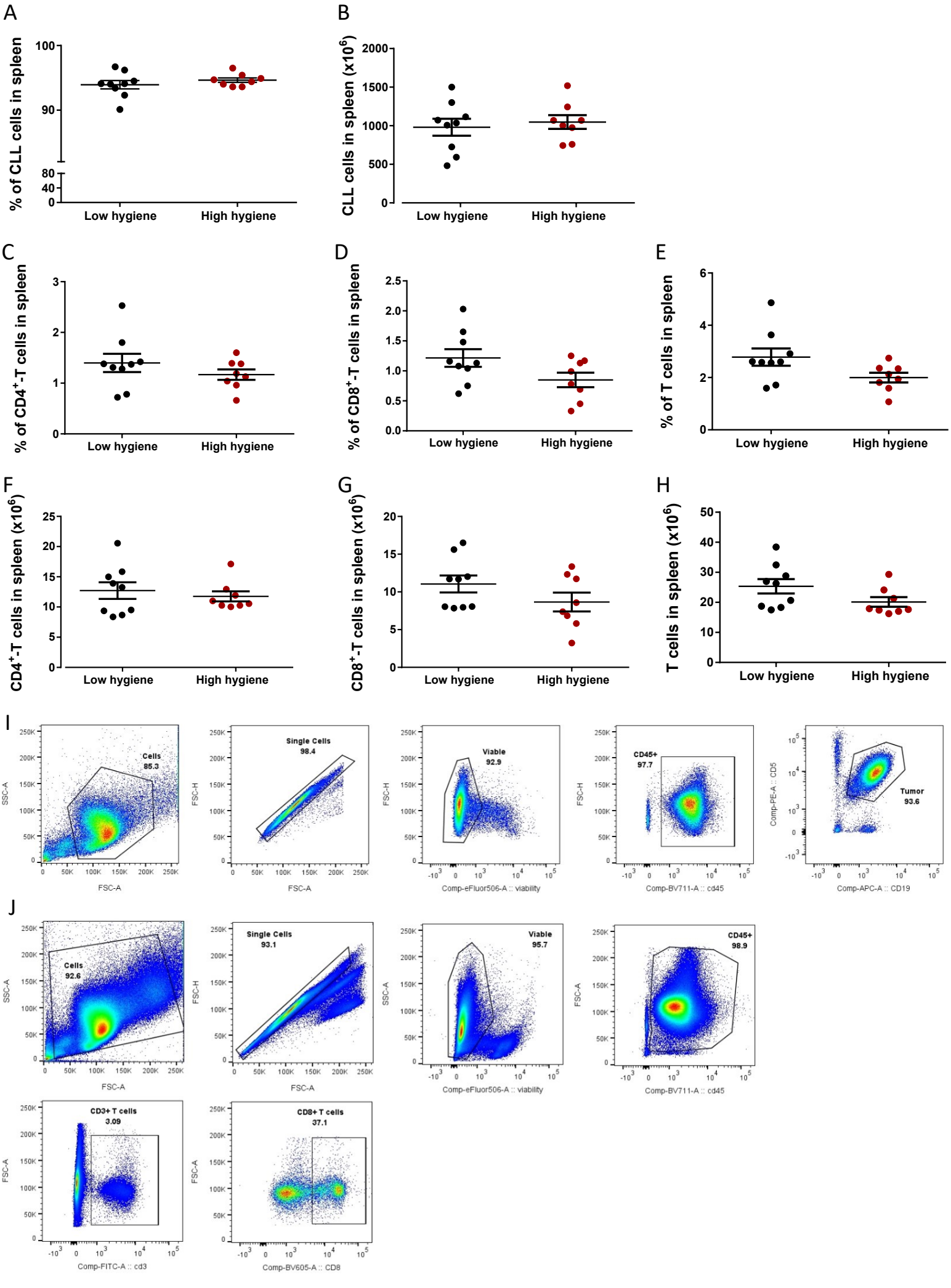

Supplemental Figure 1. A) Percentage of CLL cells (CD19+CD5+) out of CD45+ compartment in spleen. B) Absolute number of CLL cells in spleen (x10^6). C-E) Percentage of CD4+, CD8+ and CD3+ T cells in spleen out of viable compartment. F-H) Absolute number of CD4+, CD8+ and CD3+ T cells in spleen (x10^6). I) Exemplary gating strategy for CD19+CD5+ CLL cells ("Tumor"). J) Exemplary gating strategy for CD8+ T cells.

Supplemental Figure 2

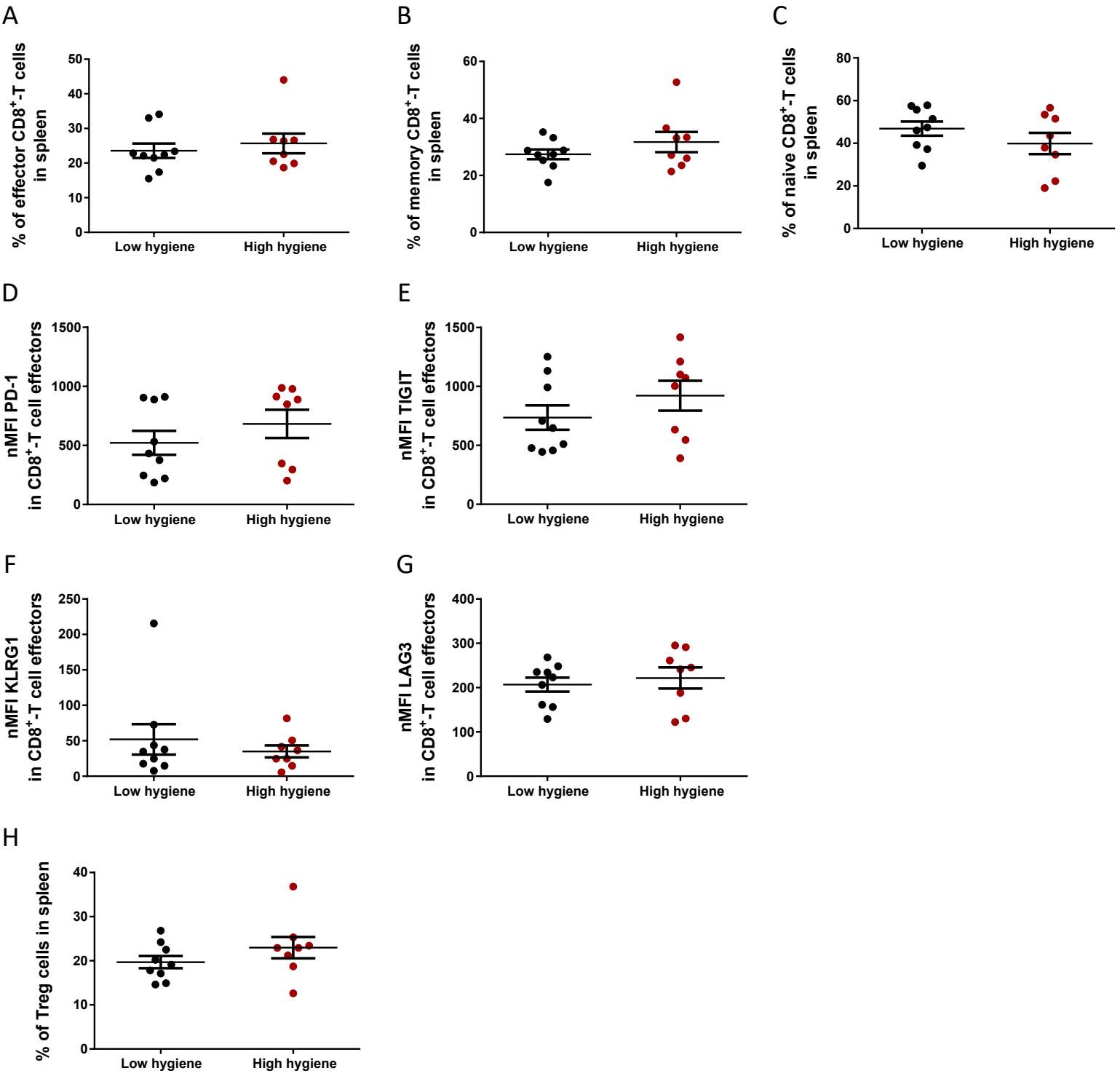

Supplemental Figure 2. A-C) Percentage of effector, memory and naive CD8+ T cells out of T cell splenic compartment. D-G) Normalized median fluorescence intensity (nMFI) of PD-1, TIGIT, KLRG1 and LAG3 in CD8+ T effector cells in t he splenic compartment. H) Percentage of FoxP3+CD25+ Treg cells out of CD4+ cells in the splenic compartment.

Supplemental Figure 3

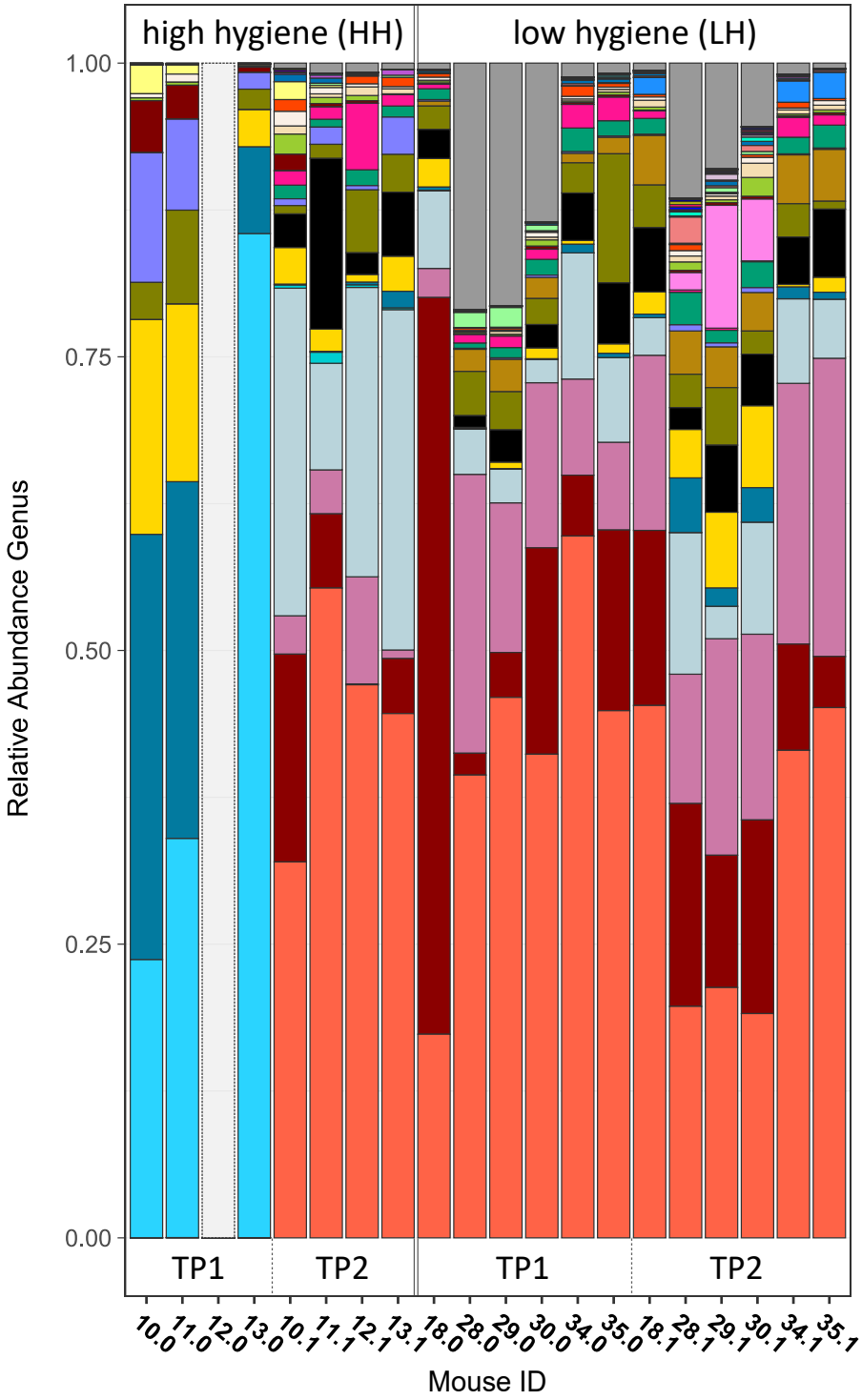

Genus

bacterial genera
with total abundance > 1%

- Unclassified
- Adlercreutzia
- Akkermansia
- 12 Alistipes
- Anaerostipes
- Anaerotruncus
- Bacteroidaceae gen. incertae sedis
- 4 Bacteroidales gen. incertae sedis
- 5 Bacteroides
- Bifidobacterium
- Bittarella
- 10 Burkholderiales gen. incertae sedis
- 13 Clostridiaceae gen. incertae sedis
- Clostridiales gen. [Clostridium/Flavonifractor]
- 15 Clostridiales gen. incertae sedis
- 14 Clostridium
- Dorea
- Dubosiella
- Eggerthella
- Enterorhabdus
- Erysipelatoclostridium
- Eubacterium
- Faecalibaculum
- Firmicutes gen. [Erysipelatoclostridium/Clostridioides]
- 11 Firmicutes gen. incertae sedis
- Flavonifractor
- 3 Helicobacter
- Hungateiclostridiaceae gen. incertae sedis
- Ileibacterium
- Intestinimonas
- 7 Lachnospiraceae gen. incertae sedis
- 9 Lactobacillus
- 2 Mucispirillum
- 1 Muribaculaceae gen. incertae sedis
- 8 Muribaculum
- Oscillibacter
- Paeniclostridium
- 6 Parabacteroides
- Proteobacteria gen. [Escherichia/Klebsiella/Shigella]
- Pseudoflavonifractor
- Romboutsia
- Ruminococcaceae gen. incertae sedis
- Staphylococcus

1-15: 15 bacterial genera with highest total rel. abundance, ranked

Supplemental Figure 4

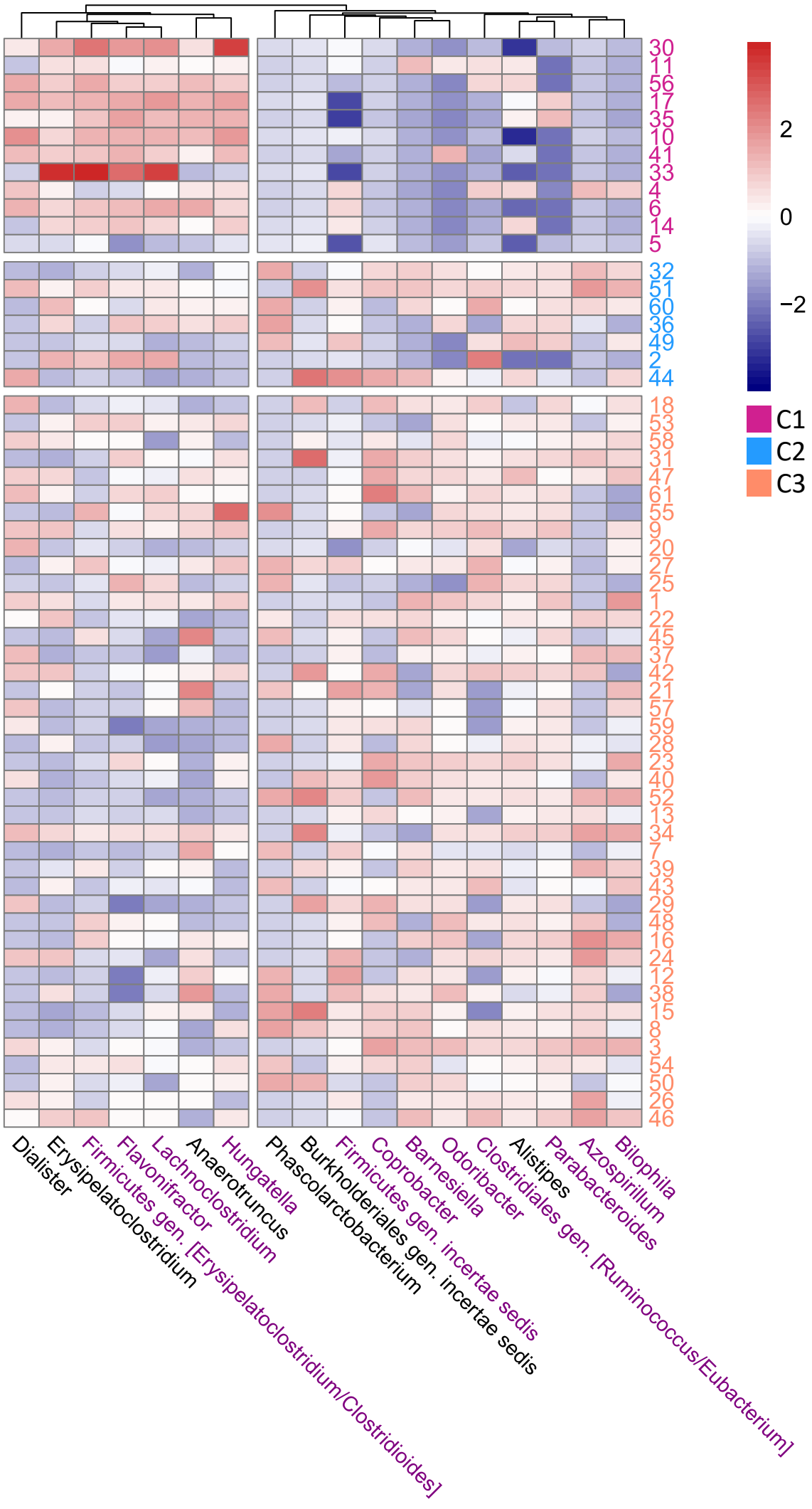

Supplemental Figure 4. Heatmap visualization of differentially abundant bacterial genera between C1 and C2, all clusters. Relative abundances of selected genera visualized for all 3 clusters. Selected genera: genera with logFC >1 enriched in C1, and twelve genera with highest logFC enriched in C2 patient samples. Patient samples (y-axis) are labeled according to the cluster membership from Figure 1. Subject 5 (from C1) was omitted from visualization due to extremely low relative abundances across all genera. Bacterial species that were found to be differentially abundant also between C1 and C3 are marked in blue. Full list of differentially abundant bacterial genera and species between C1 and C3 can be found in Supplemental Table 3. Data used for visualization were clr-transformed relative abundances. Clustered heatmap was built and visualized using kmeans clustering method from *pheatmap* function in R.

Supplemental Figure 5

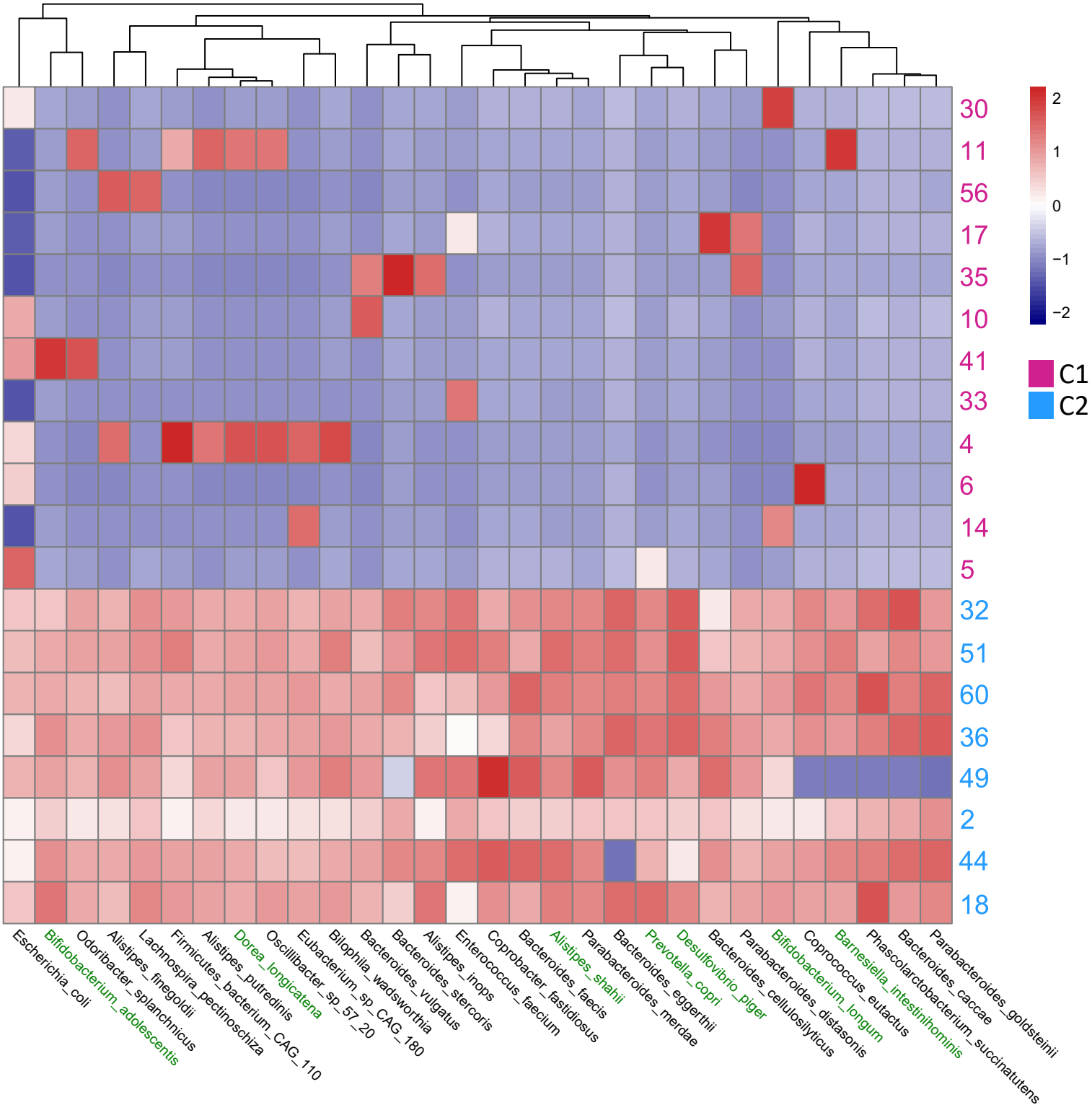

Supplemental Figure 5. Heatmap visualization of differentially abundant bacterial species between C1 and C2. Thirty bacterial species (x-axis) with highest fold change (analysis by SIAMCAT; Supplemental Table 3) were selected for visualization. Patient samples (y-axis) were labeled according to the cluster membership from Fig 1. Bacterial species enriched in patients from C2 corresponding to healthy signature identified by Gacesa et al. (12) are marked in green. Data used for visualization were clr-transformed relative abundances of bacterial species. Clustered heatmap was built and visualized using k-means clustering method from pheatmap function in R.